Characterization of the aggregates formed by various bacterial lipopolysaccharides in solution and upon interaction with antimicrobial peptides.

Gianluca Bello,[*,†] Jonny Eriksson,[‡] Ann Terry,[¶] Katarina Edwards,[‡] M. Jayne Lawrence,[†] David Barlow,[†] and Richard D. Harvey[*,†]

Institute of Pharmaceutical Science, King's College London, London, UK, Department of Chemistry - BMC, Uppsala University, Uppsala, Sweden, and Rutherford Appleton Laboratory, Harwell, Oxford, UK

E-mail: gianluca-bello@libero.it; richard.d.harvey@kcl.ac.uk

Phone: +44 (0)207 848 4831. Fax: +44 (0)207 848 4800

Supporting information

[*]To whom correspondence should be addressed
[†]Institute of Pharmaceutical Science, King's College London, London, United Kingdom
[‡]Department of Chemistry - BMC, Uppsala University, Uppsala, Sweden
[¶]Rutherford Appleton Laboratory, Harwell, Oxford, United Kingdom

SANS data

Smooth LPS 0111B4

Data for SANS measurements of Smooth LPS 0111B4 dilutions.

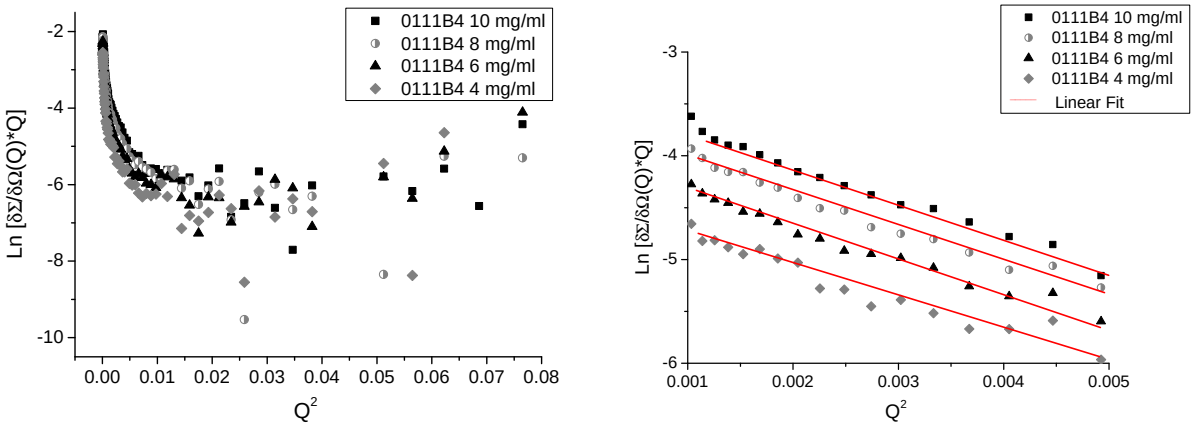

Figure 1: (A) Kratky plot of scattering data of LPS 0111B4 dilutions in 1 mM $MgCl_2$ solution at 37°C . (B) Linear curve fitting of the expanded intermediate-high Q^2 range of 0.001-0.005 of the Kratky plot.

Table 1: Values from the linear fitting of Kratky plot of LPS 0111B4 dilutions at intermediate-high Q range of 0.032-0.067.

0111B4	R^2 fit	R_g (Å)	$R = \sqrt{2} * R_g$ (Å)	M_L (Da/Å)
10 mg/ml	0.982	26.0±0.6	37	55'124 ±509
8 mg/ml	0.977	26.1±0.7	37	74'282 ±725
6 mg/ml	0.973	25.2±0.7	36	108'855 ±992
4 mg/ml	0.921	24.5±1.2	35	180'744 ±2472

Rough Ra LPS D21

Data for SANS measurements of LPS D21 dilutions.

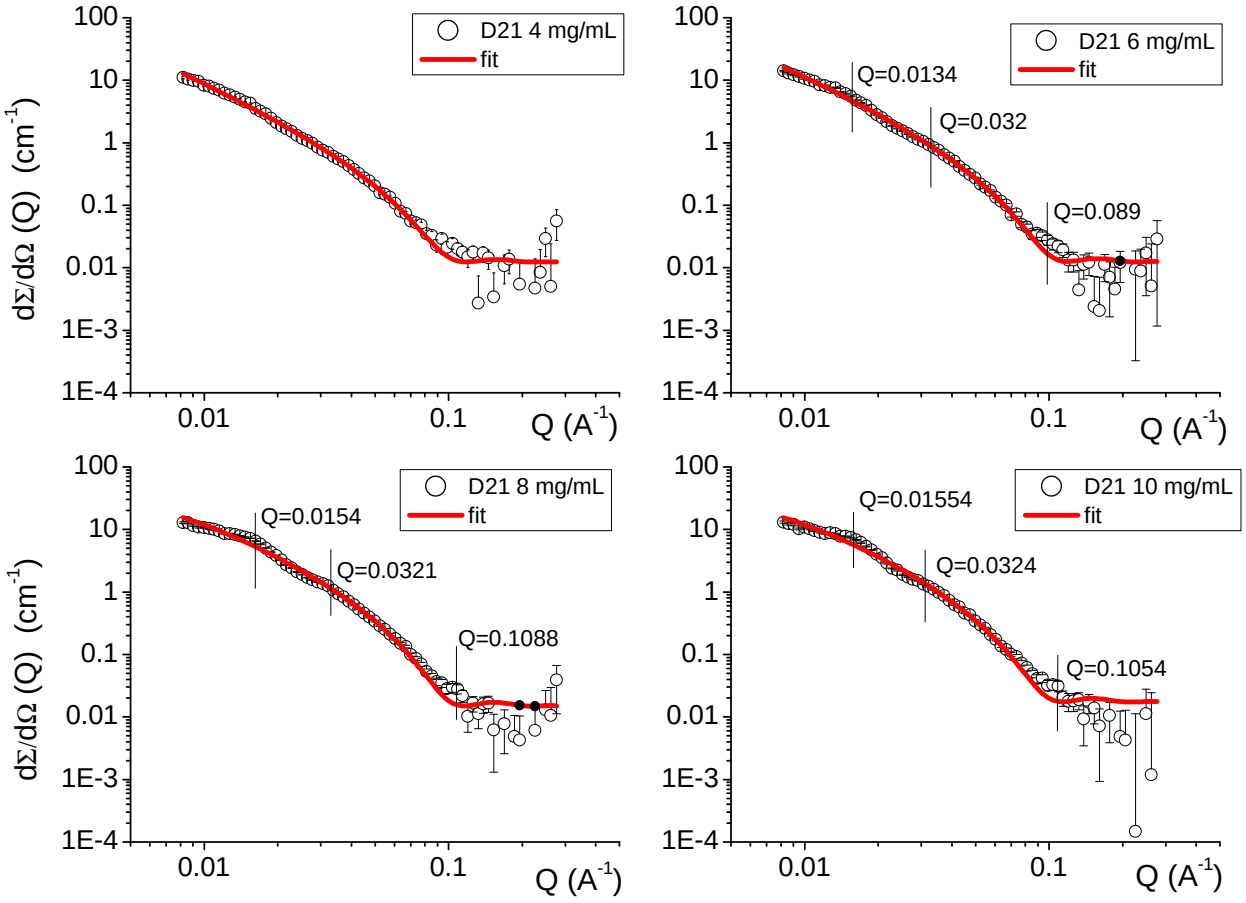

Figure 2: SANS data for LPS D21 dilutions in a 1 mM $MgCl_2$ solution at 37°C fitted as monodisperse oriented sheet shell/core/shell provided by the FISH software. The Q values reported have been considered of interest.

Table 2: Monodisperse sheet shell/core/shell model parameters obtained from the fitting of LPS D21 dilutions in a 1 mM $MgCl_2$ solution at 37°C alone, and at the concentration of 6 mg/ml in the presence of the peptide LFb at LPS/peptide ratios of 50/1 and 10/1.

D21	4 mg/ml	6 mg/ml	8 mg/ml	10 mg/ml	+ LFb 50/1	+ LFb 10/1
Scale	0.042	0.039	0.016	0.014	4.771	0.838
ϕ^a	0.00285	0.00427	0.00635	0.00768	0.00273	0.00277
t_c (Å) ^{b}	23 ±0	23 ±0	23 ±0	23 ±12	22±0	26 ±0
t_s (Å) ^{c}	17 ±0	17 ±0	18 ±0	17 ±6	16± 0	13 ±0
T (Å) ^{d}	57	57	59	57	54	52
$R\sigma$ (Å)	503	408	229	211	330	210
SSE ^{e}	3.38 e+02	6.79 e+02	1.65 e+03	1.14 e+03	1.84 e+02	2.60 e+02

^{a} calculated volume fraction from the *Scale* according to Equation 14; ^{b} core thickness; ^{c} shell thickness; ^{d} Total thickness $T = 2 * t_s + t_c$; ^{e} sum of squared errors.

Rough Rd LPS D21E7

Data for SANS measurements of LPS E7 dilutions.

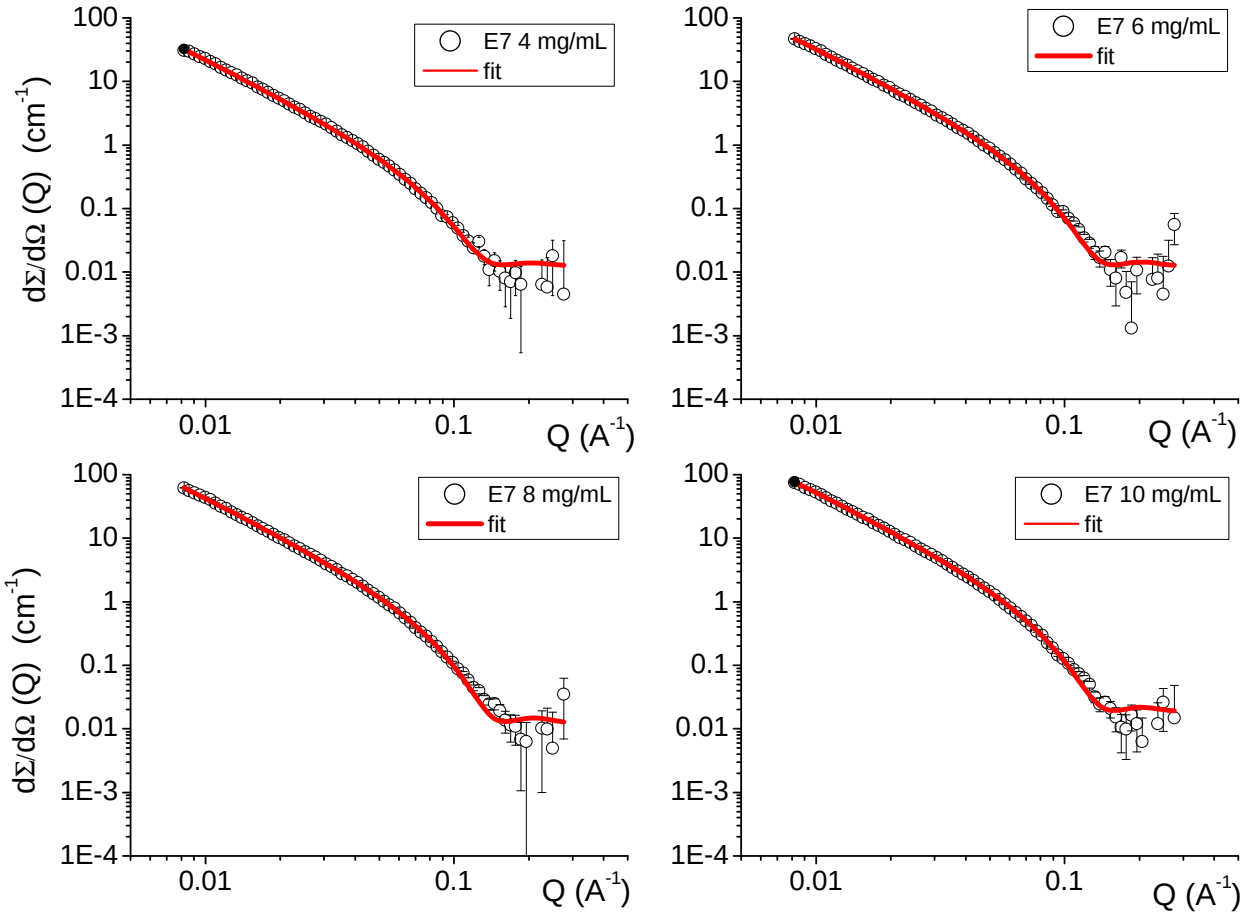

Figure 3: Monodisperse oriented sheet shell/core/shell model fitting of LPS E7 dilutions in a 1 mM $MgCl_2$ solution at 37°C .

Table 3: Parameters obtained from the monodisperse oriented sheet shell/core/shell model fitting of LPS E7 dilutions in a 1 mM $MgCl_2$ solution at 37°C .

E7	4 mg/ml	6 mg/ml	8 mg/ml	10 mg/ml
Scale factor	0.042	0.423	1.107	0.885
t_c (Å) [a]	17.25 ±7.67 e-17 [e]	17.25 ±4.83 e-17	17.04 ±1.43 e-17	17.24 ±4.79 e-14
t_s (Å) [b]	13.02 ±4.88 e-17	13.02 ±3.08 e-17	12.63 ±9.08 e-18	12.93 ±3.05 e-14
T (Å) [c]	43.29	43.29	42.30	43.10
$R\sigma$ (Å)	769.85	769.85	875.82	716.09
SSE [d]	2.14 e+02	1.39 e+02	1.74 e+02	1.22 e+02

[a] core thickness; [b] shell thickness; [c] Total thickness $T = 2 * t_s + t_c$; [d] sum of squared errors. [e] Errors quoted are those calculated from the variance-covariance matrix obtained in the least-squares fitting procedure, and in all cases, therefore, are underestimates of the true errors.

Discussion figure

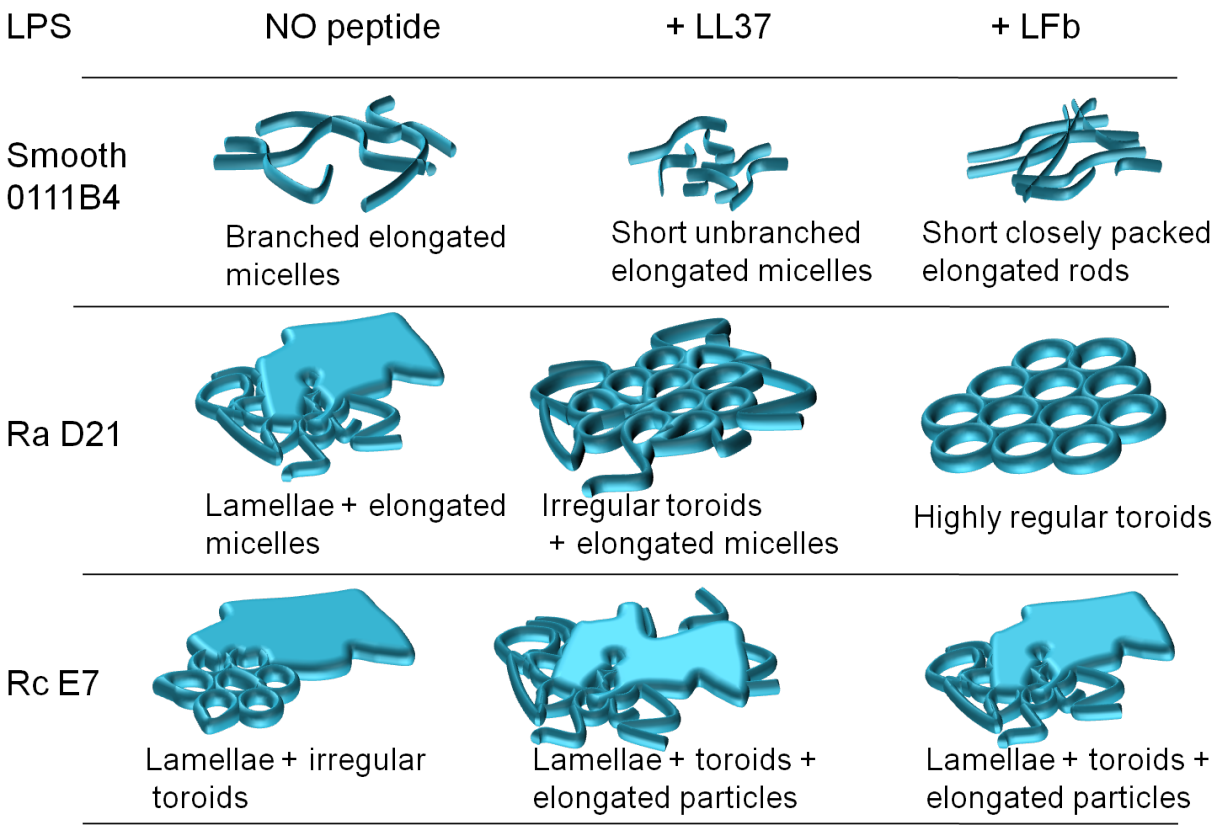

Figure 4: Representation of the aggregate structures formed by various LPS chemotypes and the effect of the peptides LL37 and LFb on the morphology of the aggregates.

SANS data analysis

Analysis of the SANS data was performed via the simple observation of the characteristic features of the scattering pattern, but also with the manipulation of the scattering curves trough mathematical approximations of SANS data, which apply particular plotting in order to determine sample parameters by approximating the characteristic scattering patterns from defined colloidal morphologies. This type of data manipulation is implemented sometimes with a more detailed analysis of the scattering curves which required the use of specific software in order to apply complex mathematical modelling to the SANS data. These models yielded more detailed information on the aggregate morphologies.

Analysis of elongated objects The Kratky-Porod worm like chain model[1–3] is used to describe elongated particles of L length by the form factor

$$\frac{\partial \Sigma}{\partial \Omega}(Q) \;=\; N\, V^2\, (\Delta\rho)^2 \;\left[\frac{2}{Q\,L}\left(S_i\,(Q\,L) - \frac{(1-cos(Q\,L))}{Q\,L}\right)\right] \tag{1}$$

and S_i is expressed by:

$$S_i(Q\,L) \;=\; \int_0^{Q\,L} \frac{sin(x)}{x} dx \tag{2}$$

Figure 5 A shows a schematic representation of an elongated object of n, l and L which

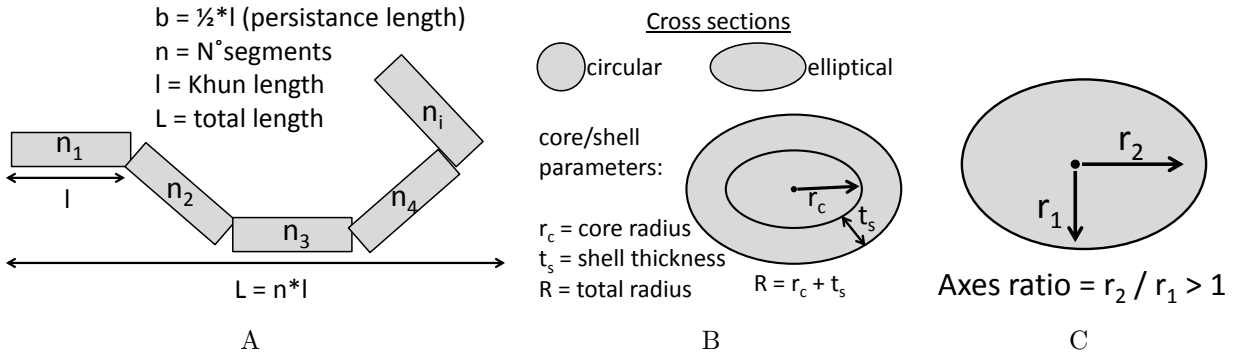

Figure 5: A) Representation of a worm like chain formed by n segments of length l. B) Possible cross sections for elongated objects with description of the core/shell cross section. C) Axial ratio in the case of an ellyptical cross section.

are the same parameters described by the Kratky-Porod model. Figures 5 B and C describe

also the possible cross sections that an elongated object can have. The cross sections can be either cylindrical or ellyptical depending upon the ratio between the X and Y radii of the section; a cross section can be also formed by an inner core and an outer shell distinguished by a r_c and a t_s. The Equation 1 is simplified for infinitely long chains in the intermediate-high Q range with limits of $Q > b^{-1}$ where b, the persistence length, is half of the l factor (see Figure 5 A), hence it becomes

$$\frac{\partial \Sigma}{\partial \Omega}(Q) \approx \frac{\pi\, c\, (\Delta\rho)^2}{N_A\, \delta^2} \times \frac{M_L}{Q} \tag{3}$$

where M_L is the mass per unit length equal to M/n and c is the concentration of solute in g/ml. In order to incorporate the cross sectional radius of gyration ($R_{g,xs}$) as finite parameter, the expression is extended considering a Guinier-like factor:

$$\frac{\partial \Sigma}{\partial \Omega}(Q) \approx \frac{\pi\, c\, (\Delta\rho)^2}{N_A\, \delta^2} \times \frac{M_L}{Q} \times \overbrace{exp\left(-\frac{Q^2\, R_{g,xs}^2}{2}\right)}^{Guinier\, factor} \tag{4}$$

Following the Equation 4, the linear plot of $ln[Q \times (\delta\Sigma/\delta\Omega)(Q)]$ vs Q^2 gives

$$slope = -\frac{R_{g,xs}^2}{2} \tag{5}$$

$$intercept = ln\left(\frac{\pi\, c\, (\Delta\rho)^2\, M_L}{N_A\, \delta^2}\right) \tag{6}$$

This approximation is valid if it is linear at high Q^2 values and for a limit of $Q \times R_{g,xs} < 1.1$; the value of $R_{g,xs}$ allows the calculation of the radius of the elongated object $R = \sqrt{R_{g,xs}}$. In addition the intercept can be used to determine the mass per unit length ${M_L}^4$ in Da/Å as

$$M_L = \frac{1000\, intercept\, \delta^2\, N_A}{\pi\, C\, (\rho_{worm} - \rho_{solvent})^2} \tag{7}$$

where C is the concentration in g/L.

Following the data approximation it is logical to try to apply a more defined mathematical

model to fit the scattering curve in order to maximise the amount of extractable information from the SANS data. The Kratky-Porod theory is at the base of the Kholodenko worm like chain models[5] used in the FISH software and applied to elongated flexible objects. Two different Kholodenko models are available whether the chain is considered as having a uniform SLD or differing SLDs between the core and the shell region (see Figure 5 B). The model with the uniform SLD presents the scale factor:

$$scale \;=\; 10^{-24}\,\phi\,(\rho_{worm} - \rho_{solvent})^2 \tag{8}$$

while the core/shell model presents a scale factor of

$$scale \;=\; 10^{-24}\,\phi_{core}\,(\rho_1 - \rho_2)^2 \tag{9}$$

and a contrast of

$$Contrast \;=\; \frac{(\rho_2 - \rho_3)}{(\rho_1 - \rho_3)} \tag{10}$$

where ρ_1, ρ_2, ρ_3 are respectively the core, shell and solvent scattering length densities in cm^{-1}.

Analysis of lamellar aggregates A lamellar aggregate is considered to be formed by at least one bilayer of amphiphiles in which the core hydrophobic region contains the acyl chains and the shell hydrophilic region is composed of the headgroups, in contact with the aqueous bulk. Such a structure could be repeated indefinitely to form stacks defined by the *d-spacing* with a core thickness t_c and a shell thickness t_s (Figure 6). In our specific case the core of the lamellae consists solely of the hydrocarbon chains of LPS while the shell of the bilayer is composed of the the Core region and eventually the O-antigen region of the oligosaccharide headgroup.

In the mathematical model provided by the FISH fitting software used for the fitting of neutron scattering data as monodisperse oriented sheet with a shell/core/shell feature

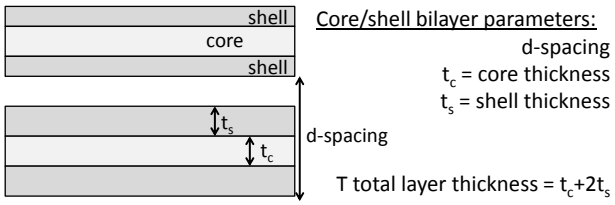

Figure 6: Representation of bilayer structure with shell/core/shell features. Shell and core have different SLDs.

(Figure 6), the neutron scattering intensity IQ is calculated as:

$$I(Q) \;=\; I(Q) + Scale \cdot L_N(Q) \cdot f^2(Q) \tag{11}$$

where Scale is the scale factor defined by the model, $L_N(Q)$ is a Lorentzian factor which considers a random orientation of the sheets and $f(Q)$ is the molecular form factor for such a model:[6]

$$f(Q) \;=\; t_c \, \frac{sin(Qt_c/2)}{Qt_c/2} \, 2t_s \, \frac{\rho_2 - \rho_3}{\rho_1 - \rho_3} \, cos(Q(t_c + t_s)/2) \, \frac{sin(Qt_s/2)}{Qt_s/2} \tag{12}$$

in which l_1 and t_s are respectively the core and the shell thickness, therefore the total thickness of a bilayer T is $T = t_c + 2t_s$; ρ_1 and ρ_2 are the scattering length densities of respectively the hydrophobic and the hydrophilic regions of the LPS molecule, whilst ρ_3 is the solvent scattering length density. The main parameters for this model are t_c and t_s, $R\sigma$ which is a parameter that describes the uniformity of an object, the contrast is expressed as

$$Contrast \;=\; \frac{(\rho_2 - \rho_3)}{(\rho_1 - \rho_3)} \tag{13}$$

and the scale factor

$$Scale\, factor \;=\; 10^{-32} \cdot \Pi \cdot (\rho_1 - \rho_3)^2 \cdot S \cdot (R\sigma)^2 \tag{14}$$

where S is the area of sheet per unit volume of sample in cm^{-1}. S is also expressed as the function

$$S = \frac{\phi}{10^{-8} t_c} \tag{15}$$

in the case of a truly infinite sheet; it is therefore possible to calculate back the volume fraction ϕ in order to check the validity of its calculated value.

References

(1) King, S. M. *Modern Techniques for Polymer Characterisation*; J. Wiley, 1999; Chapter 7, Small-Angle Neutron Scattering, pp 171–231.

(2) Pedersen, J. S.; Schurtenberger, P. Scattering Functions of Semiflexible Polymers with and without Excluded Volume Effects. *Macromolecules* **1996**, *29*, 7602–7612.

(3) Sivia, D. S. *Elementary scattering theory: for X-ray and neutron users*; Oxford, 2011.

(4) Thiyagarajan, P.; Burkoth, T.; Urban, V.; Seifert, S.; Benzinger, T.; Morgan, D.; Gordon, D.; Meredith, S.; Lynn, D. pH dependent self assembly of β-amyloid(10-35) and β-amyloid(10-35)-PEG3000. *J. Appl. Crystallogr.* **2000**, *33*, 535–539.

(5) Kholodenko, A. L. Analytical calculation of the scattering function for polymers of arbitrary flexibility using the Dirac propagator. *Macromolecules* **1993**, *26*, 4179–4183.

(6) Kotlarchyk, M.; Sheu, E.; Capel, M. Structural and dynamical transformations between neighboring dense microemulsion phases. *Phys. Rev. A: At., Mol., Opt. Phys.* **1992**, *46*, 928–939.